Supplement of Hydrol. Earth Syst. Sci., 30, 1487–1501, 2026
https://doi.org/10.5194/hess-30-1487-2026-supplement

Hydrology and Earth System Sciences
Open Access
EGU

Supplement of

A lesson in preparedness: assessing the effectiveness of low-cost post-wildfire flood protection measures for the catastrophic flood in Kineta, Greece

George Papaioannou et al.

Correspondence to: George Papaioannou (gpapaio@fmenr.duth.gr)

Supplementary Material

S1. Remote sensing analysis for the wildfire's impact on the catchment, and the flood extent

For the identification of the 2018 wildfire impacts, initially we used three Sentinel-2 (S2) MSI satellite images to capture pre-wildfire and post-wildfire conditions (1 image, and 2 images, respectively). These images were sourced from the Copernicus Open Access Hub (The Sentinels Scientific Data Hub, 2023), selected based on the ESA tiling grid with unique IDs assigned to each tile. Pre-processing was conducted in Q-GIS 3.6.3-Noosa using the semi-automatic classification plugin. This involved converting the images from digital numbers (DN) to top-of-atmosphere reflectance (TOA) and performing atmospheric correction using the DOS1 method (Barrett and Frazier, 2016). Subsequently, the study area was delineated to map burnt areas for two periods: July to August 2018 and July 2018 to October 2019, with a focus on regrown vegetation detection. Burnt area was based on the Normalized Burn Ratio (NBR) equation, employing bands B08 (NIR) and B12 (SWIR), with NBR values ranging from -1 to +1, indicating the severity of vegetation damage. The Change in Normalized Burn Ratio (Delta NBR-dNBR) method was employed then to highlight changes from the reference state, by subtracting post-wildfire NBR values from the reference NBR value of July 20, 2018 (date of the wildfire). A threshold value of +0.1 was applied to both dNBR files for each period to differentiate between burnt and unburnt areas within the study region (Rahman et al., 2018). The resulting dNBR values were scaled and classified based on burn severity ranges recommended by the United States Geological Survey (USGS), allowing for the identification of wildfire-affected areas and changes in burn severity levels over time for the studied period.

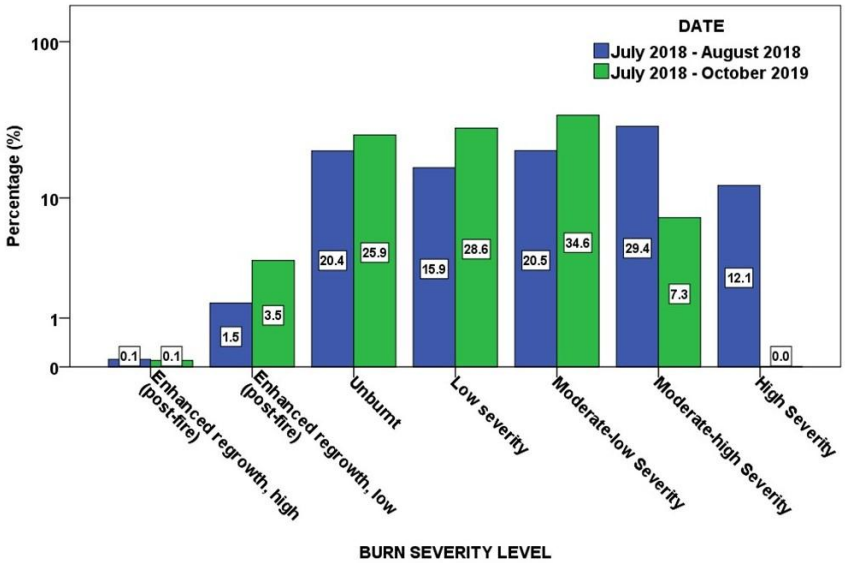

Severity Level	dNBR Range (scaled by 10^3)	dNBR Range (not scaled)
Enhanced Regrowth, high (post-fire)	-500 to -251	-0.500 to -0.251
Enhanced Regrowth, low (post-fire)	-250 to -101	-0.250 to -0.101
Unburned	-100 to +99	-0.100 to +0.99
Low Severity	+100 to +269	+0.100 to +0.269
Moderate-low Severity	+270 to +439	+0.270 to +0.439
Miderate-high Severity	+440 to +659	+0.440 to +0.659
High Severity	+660 to +1300	+0.660 to +1.300

Figure S1. Percentage extent (upper figure) of burn severity classes, according to the USGS classification (lower figure, in relation with the dNBR estimated by the remote sensing) in the Kineta catchment.

For the detection of the flood extent, only one Sentinel-2 image captured on November 25, 2019 (processing level 1C, timestamp 09:23:21:024Z) was utilized to delineate flood-inundated areas in Kineta for the event initiation on November 24, 2019. We followed the same pre-processing for this image, as in the burnt area mapping described above. To delineate water, various spectral indices (including NDWI, MNDWI, AWEI, RSWIR1, RSWIR2) were assessed utilizing S2 bands. Moreover, the SWIR2, NIR, and red bands were transformed into HSV (Hue, Saturation, Value) colours, according to the method proposed by (Pekel et al., 2014). Water indices were computed, each with manually adjusted thresholds to ensure accurate delineation. The binarization process yielded the final 'water' images. Five water indices (WIs) were computed from the S2 image dated November 25, 2019, determining the most representative threshold value for each index. Histogram analysis revealed distinct peak magnitudes, with positive values typically indicating water and negative or zero values indicating soil or terrestrial vegetation. Manual adjustment of thresholds was conducted then to refine water delineation accuracy, referencing actual images and drone videos from visual inspections conducted post-flood (Xu, 2006). Finally, each image of a distinct WI underwent binarization, assigning logical values (true) for values above the threshold and false for values below the threshold. Thus, the final 'water' images were obtained, providing us with the observed flooded area (used as ‘validation polygon’ for the flood model).

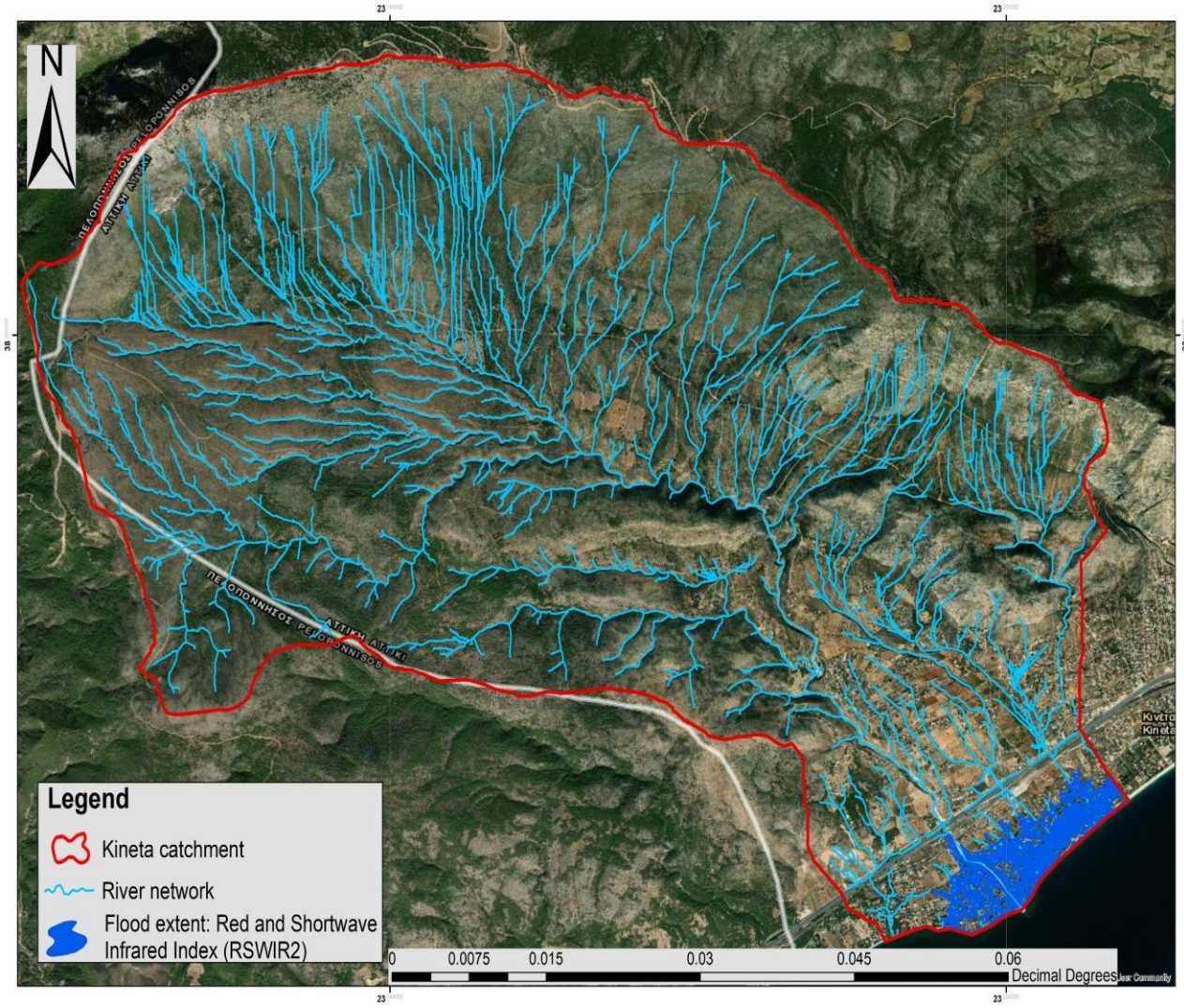

Figure S2. The flood extent of the Kineta catchment, as mapped by the remote sensing RSWIR2 index calculation. Base-map source: Imagery © 2025 NASA, Imagery Date: 08/23/2025, Map data © 2025 Google.

S2. Roughness coefficients

The Manning's roughness values were applied in a spatially distributed format in the Kineta catchment, within the HEC-RAS hydraulic model. In Table S1, the Classification Category field corresponds to the CORINE 2018 land cover categories (CLC2018), combined with the different conditions derived from the Remote Sensing observations (RS obs). So, the CLC2018 categories (e.g., Complex cultivation patterns, Coniferous forest, Mixed forest, etc.), were spatially combined with the RS observations (e.g., Enhanced re-growth high, Enhanced regrowth low, High severity, Low severity, Moderate-low severity, Moderate high severity, Unburnt), and produced the categories of the first column of Table S1. This provides spatially all the different land cover categories (according to CORINE) with their different burn/recovered status (based on the RS observations). The typical n values were determined based on the literature and test model runs.

Table S1. Manning's roughness n values for the pre-wildfire and post-wildfire scenarios. The post-wildfire scenario corresponds to the actual simulated flood of November 2019.

Classification Category (CLC2018 & RS obs)	Manning's n (pre-wildfire scenario)	Manning's n (post- wildfire scenario)
Complex cultivation patterns enhanced regrowth, high (post fire)	0.650	0.4903
Complex cultivation patterns enhanced regrowth, low (post-fire)	0.650	0.1708
Complex cultivation patterns high severity	0.650	0.0110
Complex cultivation patterns low severity	0.650	0.4903
Complex cultivation patterns moderate-low severity	0.650	0.3305
Complex cultivation patterns moderate high severity	0.650	0.1708
Complex cultivation patterns unburnt	0.650	0.6500
Coniferous forest enhanced regrowth, high (post fire)	0.800	0.6028
Coniferous forest enhanced regrowth, low (post-fire)	0.800	0.2083
Coniferous forest high severity	0.800	0.0110
Coniferous forest low severity	0.800	0.6028
Coniferous forest moderate-low severity	0.800	0.4055
Coniferous forest moderate high severity	0.800	0.2083
Coniferous forest unburnt	0.800	0.8000
Discontinuous urban fabric enhanced regrowth, low (post-fire)	0.060	0.0233
Discontinuous urban fabric low severity	0.060	0.0478
Discontinuous urban fabric moderate-low severity	0.060	0.0355
Discontinuous urban fabric unburnt	0.060	0.0600
Land principally occupied by agriculture, with significant areas of natural vegetation enhanced regrowth, high (post fire)	0.050	0.0403
Land principally occupied by agriculture, with significant areas of natural vegetation enhanced regrowth, low (post-fire)	0.050	0.0208
Land principally occupied by agriculture, with significant areas of natural vegetation low severity	0.050	0.0403
Land principally occupied by agriculture, with significant areas of natural vegetation moderate-low severity	0.050	0.0305
Land principally occupied by agriculture, with significant areas of natural vegetation moderate high severity	0.050	0.0208
Land principally occupied by agriculture, with significant areas of natural vegetation unburnt	0.050	0.0500
Mixed forest enhanced regrowth, low (post-fire)	0.800	0.2083
Mixed forest high severity	0.800	0.0110
Mixed forest low severity	0.800	0.6028
Mixed forest moderate-low severity	0.800	0.4055
Mixed forest moderate high severity	0.800	0.2083
Mixed forest unburnt	0.800	0.8000
Natural grassland enhanced regrowth, high (post fire)	0.650	0.4903
Natural grassland enhanced regrowth, low (post-fire)	0.650	0.1708
Natural grassland low severity	0.650	0.4903
Natural grassland moderate-low severity	0.650	0.3305
Natural grassland unburnt	0.650	0.6500
Road and rail networks and associated land enhanced regrowth, high (post fire)	0.013	0.0130
Road and rail networks and associated land, enhanced regrowth, low (post-fire)	0.013	0.0130

Classification Category (CLC2018 & RS obs)	Manning's n (pre-wildfire scenario)	Manning's n (post- wildfire scenario)
Road and rail networks and associated land, low severity	0.013	0.0130
Road and rail networks and associated land, unburnt	0.013	0.0130
Sea and ocean, enhanced regrowth, high (post fire)	0.070	0.0700
Sea and ocean, enhanced regrowth, low (post-fire)	0.070	0.0700
Sea and ocean, low severity	0.070	0.0700
Sea and ocean, unburnt	0.070	0.0700
Sport and leisure facilities, enhanced regrowth, high (post fire)	0.025	0.0215
Sport and leisure facilities, enhanced regrowth, low (post-fire)	0.025	0.0145
Sport and leisure facilities, high severity	0.025	0.0110
Sport and leisure facilities, low severity	0.025	0.0215
Sport and leisure facilities, moderate-low severity	0.025	0.0180
Sport and leisure facilities, moderate high severity	0.025	0.0145
Sport and leisure facilities, unburnt	0.025	0.0250
Transitional woodland/shrub, enhanced regrowth, high (post fire)	0.800	0.6028
Transitional woodland/shrub, enhanced regrowth, low (post-fire)	0.800	0.2083
Transitional woodland/shrub, high severity	0.800	0.0110
Transitional woodland/shrub, low severity	0.800	0.6028
Transitional woodland/shrub, moderate-low severity	0.800	0.4055
Transitional woodland/shrub, moderate high severity	0.800	0.2083
Transitional woodland/shrub, unburnt	0.800	0.8000
Streams	0.060	0.0950

The flood model developed in HEC-RAS combined the DEM, the spatially distributed roughness coefficient for the pre-wildfire and post-wildfire conditions, and the spatially distributed storm. For the estimation of the roughness coefficients, we combined the CORINE2018 land cover categories (complex cultivation patterns, coniferous forest, mixed forest, grasslands, road networks, etc.) with the different conditions of burn severity, as characterized from the RS results (e.g., Enhanced regrowth high, Enhanced regrowth low, High severity, Low severity, Moderate-low severity, Moderate high severity, Unburnt). For each one of these categories (all possible combinations), a Manning's n value was assigned, based on typical values from the literature (Table S1). The spatially distributed storm, namely the output from the WRF-ARW model, was inserted in HEC-RAS through the rain-on-grid routine, as spatial datasets representing different times of the storm, hourly (from 24 November 14:00:00 - 25 November 09:00:00).

S3. Hydraulic modelling / Rain-on-Grid setup

In the following table is presenting the key parameters of the Rain-on-Grid setup, including grid resolution, time step, rainfall input format, representation of hydraulic structures, and the treatment of blockage in the "reality" scenario.

Table S2. Key parameters of the Rain-on-Grid setup used in the hydraulic simulations.

Model feature	Configuration
General computational mesh resolution	General resolution = 10 m Resolution near log-erosion barriers = 5 m

	Resolution near the wooden check dams = 2 m
Initial time step	1 second
Adaptive time step configuration	Maximum Courant = 3.5 Minimum Courant = 0.5 Number of time steps before doubling = 4 Maximum number of doubling base time step = 6 Maximum number of halving base time step = 7
Downstream boundary condition	Normal depth with 0.025 friction slope
Forcing boundary condition	Gridded rainfall data derived from the Advanced Weather and Research Forecasting (WRF-ARW) v4.2 model. The data were prepared in GeoTIFF format before being imported into HEC-RAS.
Culverts	Implemented as a box culvert with the following key configurations: Entrance Loss Coefficient = 0.4 Exit Loss Coefficient = 1 Manning's n for Top and Bottom = 0.013
Bridge	Bridge blockage was simulated by modifying the terrain to reproduce the flow obstruction observed during the flood event.

S4. Flood model validation

For the validation of the hydraulic-hydrodynamic HEC-RAS model, the flooded area's polygon as obtained from the RS imagery was compared to the simulated (post-wildfire) flood inundation map. The Critical Success Index (CSI), also known as threat score (TS) was used to assess the accuracy of the simulated inundated areas against the validation polygon, according to Equation (S1):

$$\mathrm{CSI} = \frac{A}{A+B+C} \quad \text{(S1)}$$

Where:

- A is the correctly simulated flooded area (hits);
- B is the false-simulated flooded area (false alarms) – used to penalize the model's overprediction; and
- C is the flooded area that is not predicted by the model (misses).

S5. Post-wildfire Flood Protection Treatments (PFPTs) design and costs

The summary of the literature review we conducted on PFPTs, considering their main types, suitability and effectiveness (Table S3).

Table S3. Different treatment types with the most common works, and comments on site suitability and effectiveness (Papaioannou et al., 2023)

Type of Treatment	Typical works	Suitability and Effectiveness
Land – Cover-based	• Aerial Hydromulch • Ground Hydromulch • Straw Mulch • Slash Spreading • Erosion Control Mats, etc.	• Suitability: Areas with high-moderate burn severity; steep slopes; soils with high erodibility factor; low winds. • Effectiveness depends on: Proper installation, application rates, slope length and steepness, and wind conditions. Combinations of mulching and seeding is more effective in germination but not necessarily in surface cover. Wood-based mulches are equally or more effective than straw mulch in reducing post-fire erosion. Erosion Control Mats are costly solutions, with limited information about their effectiveness.
Land – Barriers	• Log Erosion Barriers • Fiber Rolls or Wattles • Silt Fences, etc.	• Suitability: Areas with high-moderate burn severity and highly erodible and water-repellent soils; slopes between 20% - 60%; accessible for maintenance and inspection. • Effectiveness depends on: Proper installation, slope, tree size and length. Barriers are more effective in low-intensity storms only. Their maintenance requires significant effort and attention. Barrier construction remains a typical hillslope treatment with better effectiveness when combined with other treatments.
Land – Seeding	• Soil Scarification • Ploughing • Seeding, etc.	• Suitability: Areas with high-moderate burn severity and highly erodible slopes; vulnerable for invasive and noxious plants spreading. • Effectiveness: While there is limited available information, seeding is inefficient in reducing sediment yield compared to no treatment. Seeding (e.g. < 60% surface cover) is not very effective in the first year after a fire and is neutral in the following seasons. Combining seeding with mulch-treatments increases the germination potential.
Land - Chemical treatments	• Polyacrylamides (PAM) • other polymers	• Suitability: There is not adequate information to generalize their site suitability. Areas with very mild rainfall events are preferred, as they boost the vegetation development fast. • Effectiveness: Very few cases report their effectiveness, with no effects found on runoff and little erosion reduction achieved.
Channel - Barriers	• Check dams • In-Channel Tree Felling • Grade Stabilizers • Stream Channel Armoring • Channel Deflectors • Debris Basins, etc.	• Suitability: Areas with high burn severity; smooth slopes where sediment storage can be achieved; with <20 % ground cover; small catchments and drainage areas; where construction, maintenance, and inspection is accessible; high-risk value (road crossing, sensitive aquatic species) and need to protect the downstream areas. • Effectiveness: Channel barriers are more effective in smooth slopes, when used in series, and for mild storms and flows. They can reduce most of the runoff and also significant amounts of erosion, but they have short-term effectiveness and require maintenance following runoff events. Debris basins are expensive treatments.
Road and Trail	• Outsloping • Rolling Dips • Overflow Structures • Culvert Modification • Trail Stabilization, etc.	• Suitability: Areas prone to flow concentration (e.g. mild slopes, bad drainage with undersized culverts) that need immediate protection from floods (important access, infrastructure, vulnerability, etc.). • Effectiveness: Limited data suggest that if properly designed and installed correctly, they provide significant benefits in terms of discharge, reduced sediment delivery to stream channels and less road maintenance.

For the Kineta catchment, we designed a series of LEBs and WCD, as shown in the Figure below.

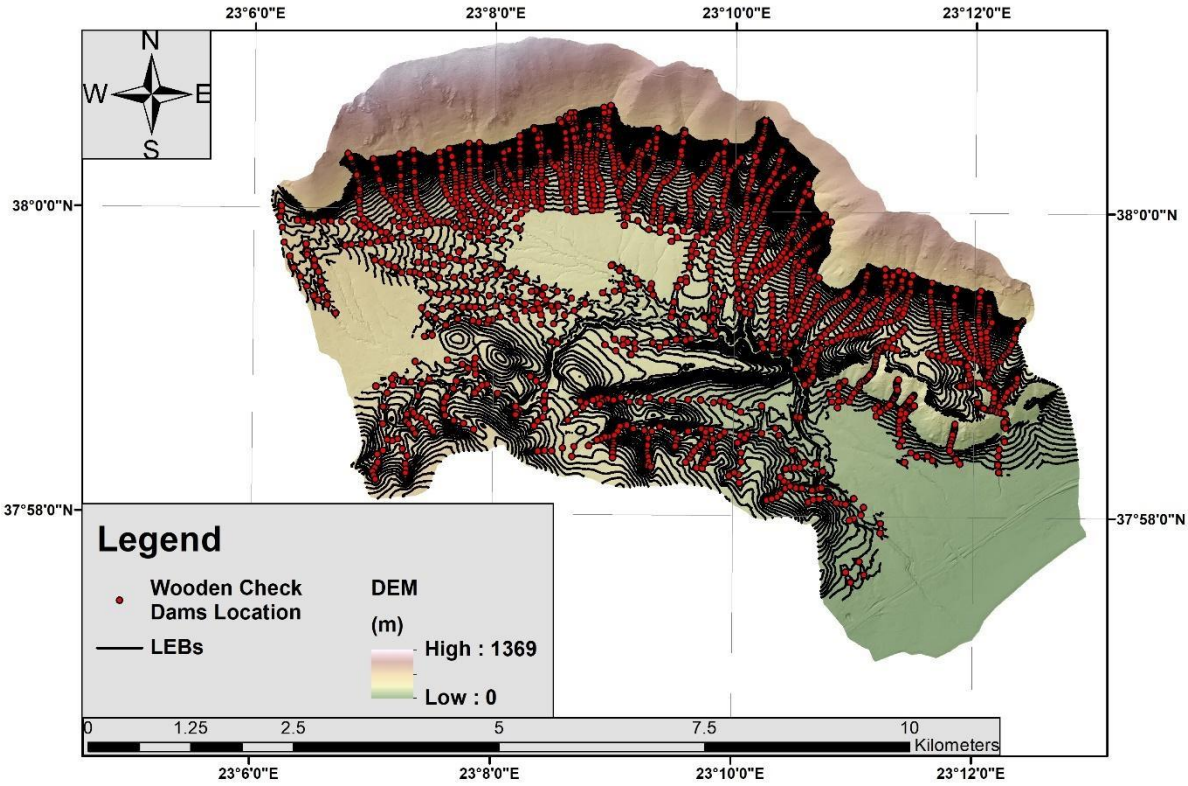

Figure S3. The terrain of the study area [adapted from: National Cadastre and Mapping Agency S.A. (NCMA, 2021)] under the hypothetical PFPT scenario, as we recommend that their placement should have been applied after the wildfire event. The map shows the locations of the installed LEBs and wooden check-dams.

Terrain modification:

A central part of this work was to run the hydraulic model HEC-RAS with a terrain reflecting the protection scenario with the spatially designed PFPTs in place.

In order to incorporate the PFPTs (log-erosion barriers (LEBs) and wooden check-dams (WCD)) of Fig.S3 in the terrain model, we used the R packages 'terra' to analyze rasters, 'sf' to analyze vectors and 'smoothr' for lines smoothing.

First, we exported the PFPT layout (Fig. S3) as a high-resolution raster mask. Using the R package 'terra', we loaded the original digital elevation model (DEM) and overlaid the PFPT raster, adjusting elevation values where barriers and check-dams were to be installed. For each LEB, we raised the DEM by 0.2 m along the contour lines at 10 m spacing; for each WCD, we inserted 1 m high linear features within stream channels at specified intervals. Next, the 'sf' package parsed the vector data, point and line shapefiles representing PFPT locations, allowing precise georeferencing of structure footprints and extents. Finally, to avoid artificial hydrological artifacts caused by unnaturally jagged barrier alignments, or odd curves in the LEBs as they followed the contours of the DEM, we applied 'smoothr' to gently smooth linear features, preserving their designed geometry while ensuring flow continuity in the hydraulic mesh. The result is a modified terrain surface that realistically incorporates PFPT elevations and

geometries, ready for HEC-RAS's rain-on-grid simulation, thus capturing how these treatments divert, slow, and attenuate post-fire flood flows.

Cost analysis

The following Table provides the cost breakdown of the unit costs for the designed PFPTs.

The total cost of a wooden check dam was initially estimated at 172€, covering direct labor and material expenses. However, when including the overhead and contractor's profit margin and the VAT, the final cost rises to approximately 252€, in alignment with recent official works conducted by the Forestry Agency of Alexandroupolis following the Evros wildfire. The same cost-upscaling approach (including overheads, contractor profit, and VAT) was consistently applied to the estimation of log-erosion barrier (LEB) costs. Thus, the final PFPTs cost, including the overhead and contractor's profit margin and the VAT, is €5,05 mil.

Table S4. Analysis of the cost components for log-erosion barriers (LEBs) and wooden check-dams, in values of €2023.

Logging costs (for pine-trees 2m long x 0.2m diameter)
Timber cost: 7.99€
Increase 10% for burnt sites: 0.80€
Increase 10% due to execution by the same work group: 0.80€
Allowance 5% for travel expenses for a distance of 0-50km: 0.40€
Good performance bonus 5%: 0.40€
Employer's Insurance 24.44%: 2.54€

Logging cost: 12.93€/m^3
Displacement and transport costs (for pine-trees 2m long x 0.2m diameter)
Transport cost for distances less than 200m: 8.98€
Increase 10% for burnt sites: 0.90€
Increase 10% due to execution by the same work group: 0.90€
Allowance 5% for travel expenses for a distance of 0-50km: 0.44€
Good performance bonus 5%: 0.45€
Employer's Insurance: 24.44% 2.85€

Transport costs: 14.53€/m^3
Estimation of LEBs construction cost per meter installed
Volume of a unit log (1m long x 0.2m diameter): 0.0314
Increase 10% for losses coverage and supporting brackets: 0.0345
Volume per meter installed: 0.066m3/m
Logging cost = 12.93€/m^3 · 0.066 m^3/m = 0.85€/m
Transport cost = 14.53€/m^3 · 0.066 m^3/m = 0.96€/m
Labour cost of an unskilled worker for digging, construction and installation 3.06€/m
----

Total cost per meter of LEBs installed: 4.87€/m
Estimation of wooden check-dam cost per square meter installed
The volume of timber required for a typical trapezoid wooden check-dam, using unit logs of typical dimensions as above, and supporting brackets and a log, tied with wires is estimated to be 1.635m^3 Logging cost = 12.93€/m^3 · 1.635m^3 = 21.14€/wooden check-dam Transport cost = 14.53€/m^3 · 1.635m^3 = 23.76€/wooden check-dam Labour cost of an unskilled worker and a logger for tools, digging, construction and installation 172.38€/m ---------- **Total cost of a wooden checked-dam of open surface of 3.5m^2 = 172.38/ 3.5 = 49.25 €/m^2**

S6. Direct flood damage cost

Here we outline the detailed approach for the estimation of the direct flood damage costs, for the "reality" *scenario, Post-wildfire, No PFPTs*, as an example.

First, the part of the Kineta town that was affected by the flood (namely the area within the validation polygon) was exported as an image. This was then used as an input to the AI tool "Segment Anything Model" (SAM) (Kirillov et al., 2023), a widely used application for image segmentation. The SAM uses a database of over 1billion masks on 11million licensed and privacy respecting images, to distinguish elements within new images (zero-shot segmentation) (Baziak et al., 2024; He et al., 2024). So, the SAM delineated the properties affected within the flood-affected area, namely, the residential homes, commercial buildings, and agricultural fields. As a cross-check, a human check-counting was also performed by navigating in Google Street Maps and comparing the results to ensure that the identified elements were complete and correctly counted (Fig.S4 and Table S4).

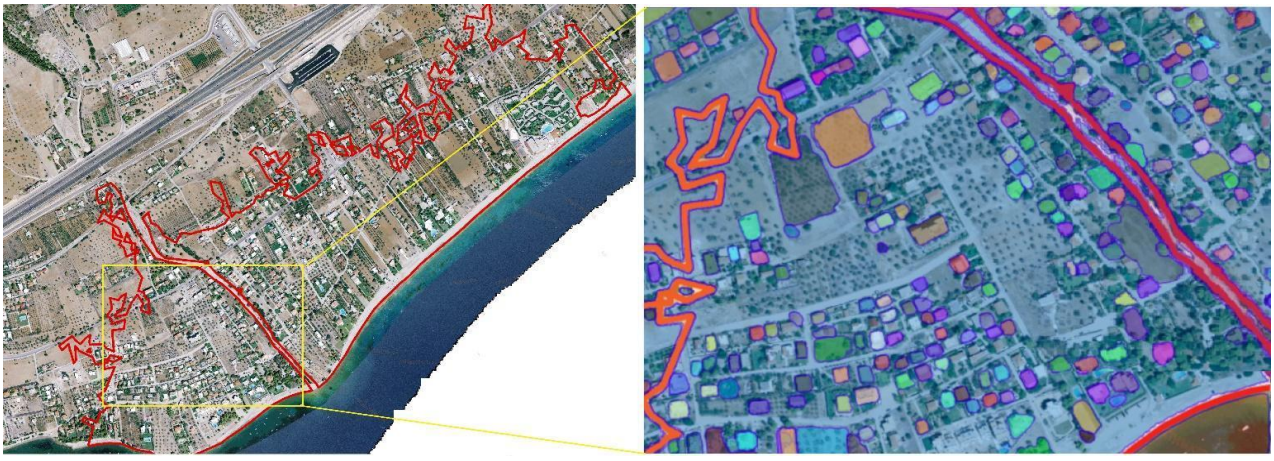

Figure S4: The affected properties from the flood of November 2019 in Kineta (left). In the right is an indicative detail (a zoomed part), showing the initial delineation of the 'house' elements by SAM, before the final human check, resulting the final numbers of Table S5. Base-map source: Imagery © 2025 NASA, Imagery Date: 08/23/2025, Map data © 2025 Google.

The counted affected elements from the flood are shown in Table S4, along with the approach followed to estimate the damages caused. In particular, to estimate the damage in residential homes, we used data from a relevant report of the (Hellenic Association of Insurance Companies, 2024). According to this report the average damage to homes from heavy precipitation in 2019 is 3,393€, which for the 541 counted houses damaged, translates into a total cost of 1,835,613€, and 2,095,531€ in 2023 value (considering the Greek cumulative inflation factor of 1.142 (Greece Inflation Rate 1960-2024, 2024). With regard to the impact of heavy precipitation on businesses, according to the same data, the average loss in 2019 was 21,203€. If we use this figure as an approximation for the average damage suffered by Kineta hotels, we have a total cost of 339,248€, which is 387,285€ in 2023 value.

According to the visual inspection study on the aftermath of the November 2019 flood of Kineta, extended damages were reported to private vehicles (iefimerida.gr, 2024; Lekkas et al., 2019). The average number of private vehicles is estimated to be 1.2 per household, and the average insurance coverage is around 1100€. So, for the affected households and vehicles, the total cost is estimated to be 714,120€ in 2023 value.

For the estimation of the direct costs of floods on agricultural fields in Kineta, Greece, we focused on the necessary cleanup expenses, as no direct loss of profits from production was incurred due to it being November when the fields were not cultivated. The total area affected by flooding, based on the flood model's simulation results, was 595,246m², with around 65% (386,910m²) being agricultural land. The cost estimation involved calculating the labour costs for an unskilled worker, tasked with tools handling, transportation, the drainage and the removal of sediments such as mud and wood debris. The typical hourly wage is 6.43€ and given that a worker could clean approximately 20m² per hour, a total of 19,346 hours was required for the entire affected area. Consequently, the estimated total labour cost for drainage and sediment removal in the agricultural fields amounted to approximately 124,392€ in 2023 value (Greek Ministry of Environment and Energy, 2023; Koudoumakis et al., 2024).

For the calculation of the economic losses due to a blocked highway from flooding, we used a general estimation model (Eq. S2) which takes into account factors like the daily vehicle traffic, the additional distance of detour, vehicle operating costs, additional travel time, and the economic value of time and goods affected (Dutta et al., 2003; Fletcher and Ekern, 2021; McCarthy, 2001; Pregnolato et al., 2017; US Department of Transportation, 2016).

$$E = (V \times D \times Ct) + (T \times Cg) + I\ , \qquad \text{(S2)}$$

Where:

- V is the daily vehicle traffic (number of vehicles per day).
- D is the additional distance of the detour (in kilometres).
- Ct is the cost per vehicle per km (considering fuel, wear and tear, and other operating costs).
- T is the additional travel time caused by the detour (in hours).
- Cg is the cost per hour per vehicle (valuing the time of the passengers and goods).
- I represents any indirect costs such as loss of revenue, long-term economic impacts, etc.

For the case of Kineta, we assumed typical traffic data for the closed section of Athens-Corinth highway, for a working day. This is approximately 10,000 vehicles per day, with 25% being commercial vehicles. The detour caused an extra 2km and an additional 30 minutes of travel time for all vehicles. The direct costs were computed by assigning an

operational cost of 0.5€/km for private vehicles and 0.8€/km for commercial vehicles, along with a value of time at 15€/hour for private vehicles and 50€/hour for commercial ones. By applying these values in Equation (S2) the total economic loss per day was calculated at 130,250€. No indirect costs considered due to data limitations (so, I=0). The road closure of the section of Athens-Corinth highway in the north of Kineta town lasted for two days (Greek Parliament, 2019; Protothema, 2019). Thus, the total cost was estimated to 260,500€ (in 2023 value).

Table S5: Estimating the cost of the flood damages per category of affected properties and infrastructure, for the "reality" scenario: Post-wildfire, No PFPTs.

Affected Properties and infrastructure	Quantity / Extent	Cost estimation approach	Estimated value (€ of 2023)
Residential homes	541	Based on the average damage cost to homes from heavy precipitation in 2019 as reported by the Hellenic Association of Insurance Companies	2,095,531
Commercial buildings (hotels)	16	Based on the 2019 average loss figure for businesses affected by heavy precipitation, also provided by the Hellenic Association of Insurance Companies	387,285
Private Vehicles	649.2	Based on the 2019 average loss figure for vehicles affected by natural disasters according to the Hellenic Association of Insurance Companies	714,120
Agricultural fields	386,910 m^2	Here, our approach focused on labour costs for cleanup and restoration, considering no direct profit loss from production, and was based on the costs for an unskilled worker to clear mud and debris, with an estimated area coverage rate and hourly wage.	124,392
Blocked highway	2 days	The estimation was based on general estimation formula that account for increased travel distance and time due to detours, with specific costs assigned per kilometer and per hour for private and commercial vehicles	260,500
Infrastructure	Roads, streams, land, drainage	Official estimated costs from the Region (Prefecture) of West Attica's Technical Works Observatory	21,643,068
Total Damage Cost			**25,224,897**

The reported expected reimbursements for the Kineta's flood to the local affected population was 3,500,000€ (iefimerida.gr, 2024). Adding to that, the flood caused significant damages to the local infrastructure (last row of Table 2), including costs for cleaning the streams from sediments (increased volumes due to the wildfire), works of land stabilization, restoration of the road network and the drainage network (Lekkas et al., 2019). As reported by the Region (Prefecture) of West Attica's Technical Works Observatory, the total repair costs for these damages reached 18,950,000€ (2021), i.e., 21,643,068€ in 2023 value (West Attica Region, 2021). So, our total estimated cost (€25.22mill.) is very close to those reported costs (€3.5mill. + €21.63mill. = €25.14mill.).

The same process was followed to estimate the flood damage costs for the other two scenarios, as summarized in Table S6 below.

Table S6: Estimates direct flood damage cost under the three scenarios explored.

Affected Properties and infrastructure	Pre-wildfire, No PFPTs (wildfire effect scenario)		Post-wildfire, No PFPTs (reality scenario)		Post-wildfire, With PFPTs (protection scenario)	
	Quantity / Extent	Estimated value (€ of 2023)	Quantity / Extent	Estimated value (€ of 2023)	Quantity / Extent	Estimated value (€ of 2023)
Residential homes	412	1,595,857	541	2,095,531	405	1,568,743
Commercial buildings (hotels)	16	387,285	16	387,285	14	338,874
Private Vehicles	495	320,055	650	714,120	486	315,511
Agricultural fields	295,701 m^2	95,068	386,910 m^2	124,392	290,923 m^2	93,532
Blocked highway	2 days	260,500	2 days	260,500	2 days	260,500
Infrastructure	Roads, streams, land, drainage	16,429,135	Roads, streams, land, drainage	21,643,068	Roads, streams, land, drainage	16,273,769
Total Damage Cost:		**19,087,901**		**25,224,897**		**18,850,929**

S7. Hydraulic model extended results

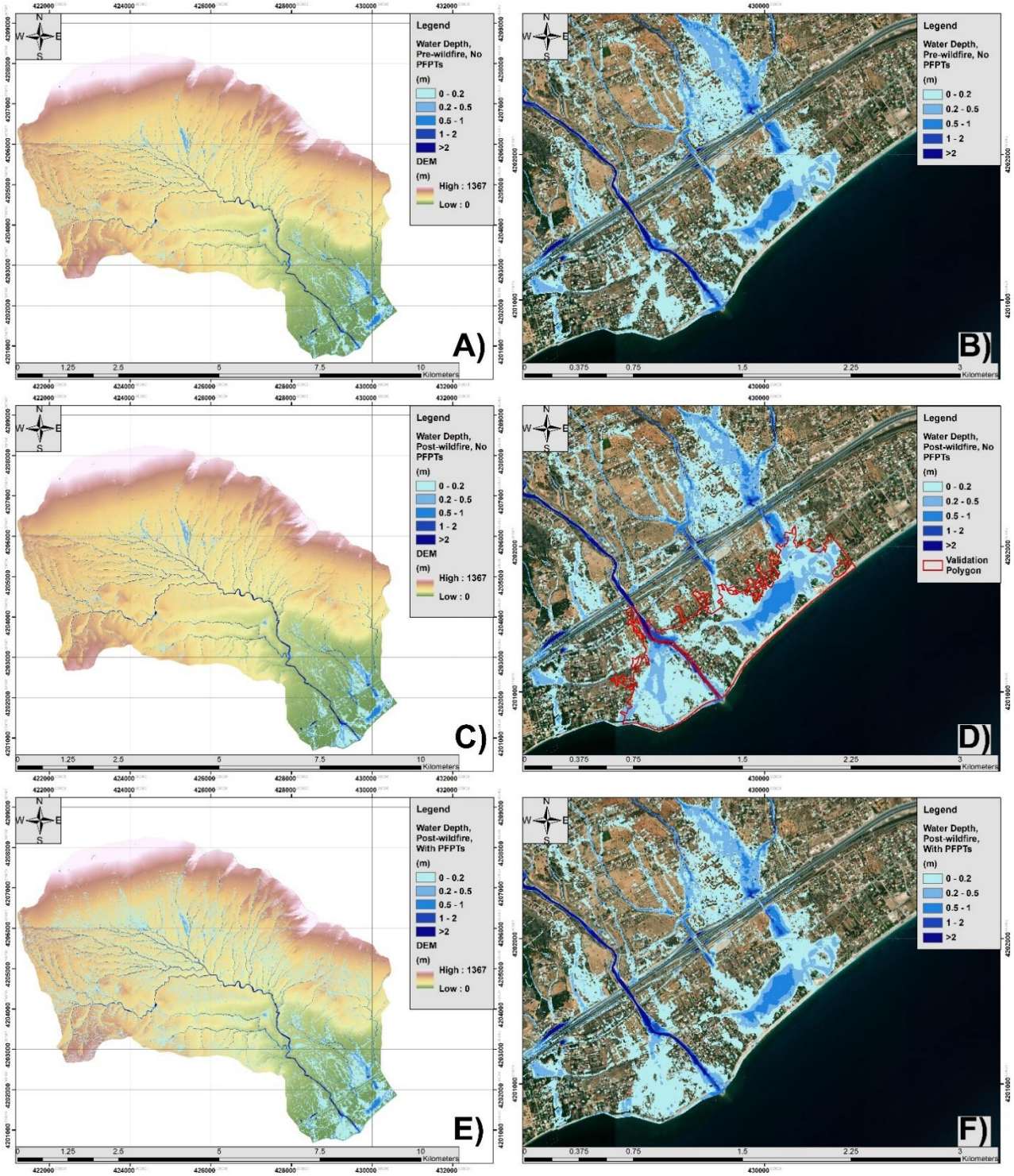

Figure S5: The extent of the flood in Kineta catchment (A),(C),(E) and the water extent and depth in the Kineta town (B),(D),(F). These are shown for the hypothetical Pre-wildfire scenario (A),(B); the real Post-wildfire, No PFPTs scenario (C),(D); and the hypothetical Post-wildfire, With PFPTs scenario (E),(F), respectively. The red "validation polygon" in

Fig.S4D represents the boundary of the water extent as resulted from RS analysis. Base-map source: Imagery © 2025 NASA, Imagery Date: 08/23/2025, Map data © 2025 Google.

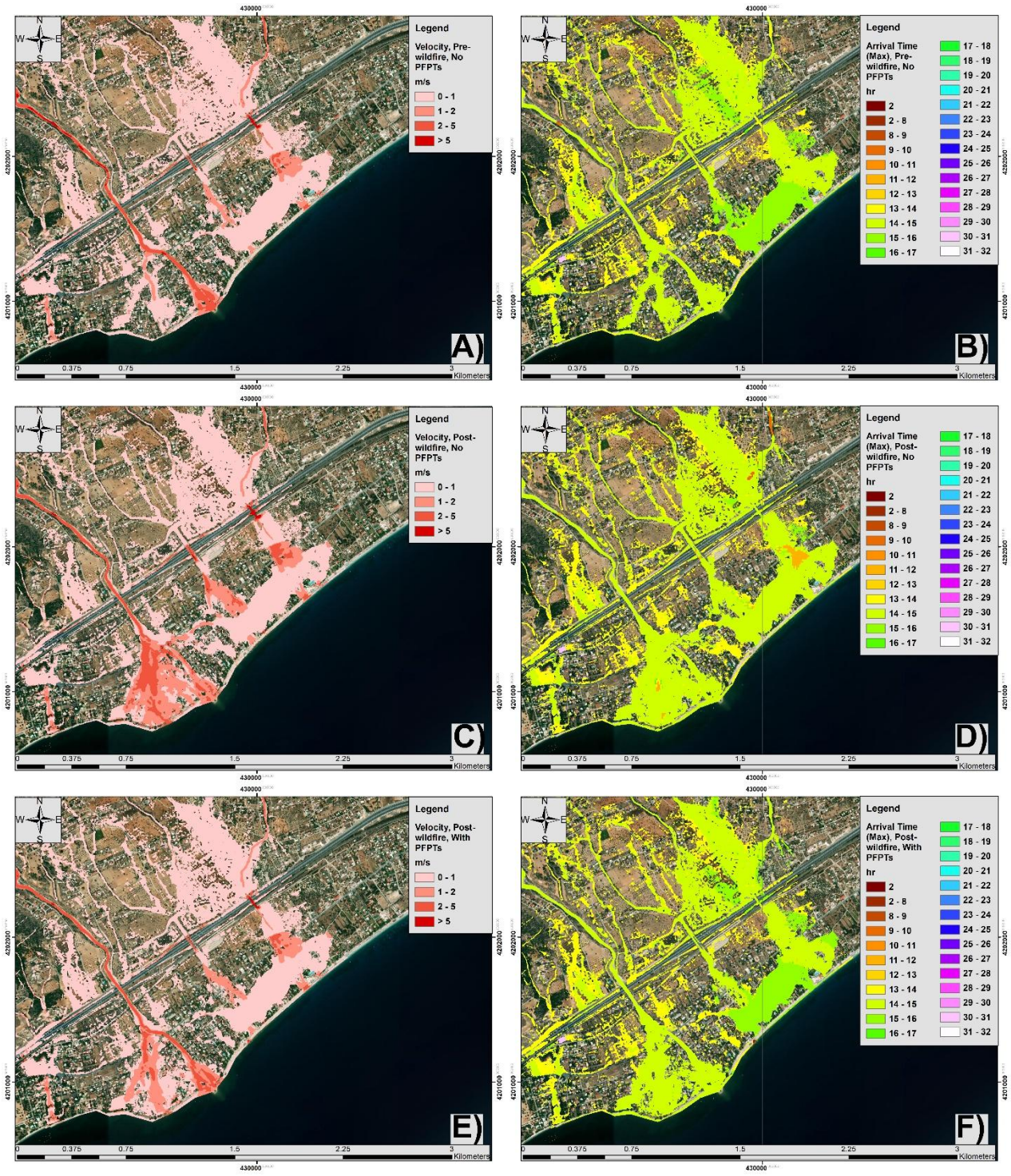

Figure S6: The water velocity (A),(C),(E), and the flood maximum arrival time in the Kineta town (B),(D),(F). These are shown for the hypothetical Pre-wildfire scenario (A),(B); the real Post-wildfire, No PFPTs scenario (C),(D); and the hypothetical Post-wildfire, With PFPTs scenario (E),(F), respectively. Base-map source: Imagery © 2025 NASA, Imagery Date: 08/23/2025, Map data © 2025 Google.

References

Barrett, D. C. and Frazier, A. E.: Automated Method for Monitoring Water Quality Using Landsat Imagery, Water, 8, 257, https://doi.org/10.3390/w8060257, 2016.

Baziak, B., Bodziony, M., and Szczepanek, R.: Mountain Streambed Roughness and Flood Extent Estimation from Imagery Using the Segment Anything Model (SAM), Hydrology, 11, 17, https://doi.org/10.3390/hydrology11020017, 2024.

The Sentinels Scientific Data Hub: https://scihub.copernicus.eu/maintenance.html#/home, last access: 2 February 2023.

Dutta, D., Herath, S., and Musiake, K.: A mathematical model for flood loss estimation, Journal of Hydrology, 277, 24–49, https://doi.org/10.1016/S0022-1694(03)00084-2, 2003.

Fletcher, D. R. and Ekern, D. S.: Transportation System Resilience: Research Roadmap and White Papers, Transportation Research Board, Washington, D.C., https://doi.org/10.17226/26160, 2021.

Greek Ministry of Environment and Energy: Study on soil-erosion and flood protection works at the burnt area of the Avantas catchment and surounding settlements. Decentralized Administration of Macedonia and Thrace. (in Greek), 2023.

Greek Parliament: Greek Parliament Minutes of the 27 November 2019, Athens, Greece, 2019.

He, Y., Wang, J., Zhang, Y., and Liao, C.: An efficient urban flood mapping framework towards disaster response driven by weakly supervised semantic segmentation with decoupled training samples, ISPRS Journal of Photogrammetry and Remote Sensing, 207, 338–358, https://doi.org/10.1016/j.isprsjprs.2023.12.009, 2024.

Hellenic Association of Insurance Companies: 1993 – 2023: Analysis of the damages of disastrous events, Athens, Greece, 2024.

The causes of the disaster in Kineta: https://www.iefimerida.gr/ellada/aytopsia-lekka-stin-kineta-aitia-tis-katastrofis, last access: 27 April 2024.

Kineta: 3.5 million euro needed for the flood damage recovery: https://www.iefimerida.gr/ellada/kineta-erga-35-ekat-eyro-gia-apokatastasi-zimion, last access: 27 April 2024.

Kirillov, A., Mintun, E., Ravi, N., Mao, H., Rolland, C., Gustafson, L., Xiao, T., Whitehead, S., Berg, A. C., Lo, W.-Y., Dollár, P., and Girshick, R.: Segment Anything, https://doi.org/10.48550/arXiv.2304.02643, 5 April 2023.

Koudoumakis, P., Keramitsoglou, K., Protopapas, A. L., and Dokas, I.: A general method for multi–hazard intensity assessment for cultural resources: Implementation in the region of Eastern Macedonia and Thrace, Greece, International Journal of Disaster Risk Reduction, 100, 104197, https://doi.org/10.1016/j.ijdrr.2023.104197, 2024.

Lekkas, E., Spyrou, N., Filis, C., Diakakis, M., Vassilakis, E., Katsetsiadou, A., Milios, D., Arianoutsou, M., Faragitakis, G., Christopoulou, A., and Antoniou, V.: The November 25, 2019 Kineta (Western Attica) Flood., Athens, Greece, 2019.

Greece Inflation Rate 1960-2024: https://www.macrotrends.net/global-metrics/countries/GRC/greece/inflation-rate-cpi, last access: 27 April 2024.

McCarthy, P. S.: Transportation Economics: Theory and Practice : a Case Study Approach, Blackwell Publishers, 620 pp., 2001.

NCMA (2021). National Cadastre and Mapping Agency S.A. (NCMA).

Papaioannou, G., Alamanos, A., and Maris, F.: Evaluating Post-Fire Erosion and Flood Protection Techniques: A Narrative Review of Applications, GeoHazards, 4, 380–405, https://doi.org/10.3390/geohazards4040022, 2023.

Pekel, J.-F., Vancutsem, C., Bastin, L., Clerici, M., Vanbogaert, E., Bartholomé, E., and Defourny, P.: A near real-time water surface detection method based on HSV transformation of MODIS multi-spectral time series data, Remote Sensing of Environment, 140, 704–716, https://doi.org/10.1016/j.rse.2013.10.008, 2014.

Pregnolato, M., Ford, A., Wilkinson, S. M., and Dawson, R. J.: The impact of flooding on road transport: A depth-disruption function, Transportation Research Part D: Transport and Environment, 55, 67–81, https://doi.org/10.1016/j.trd.2017.06.020, 2017.

Protothema: Storm "Girionis": Flooded Kineta and Katerini - Closed the Athens-Corinth Highway, ProtoThema, 25th November, 2019.

Rahman, S., Chang, H.-C., Hehir, W., Magilli, C., and Tomkins, K.: Inter-Comparison of Fire Severity Indices from Moderate (Modis) and Moderate-To-High Spatial Resolution (Landsat 8 & Sentinel-2A) Satellite Sensors, in: IGARSS 2018 - 2018 IEEE International Geoscience and Remote Sensing Symposium, IGARSS 2018 - 2018 IEEE International Geoscience and Remote Sensing Symposium, 2873–2876, https://doi.org/10.1109/IGARSS.2018.8518449, 2018.

US Department of Transportation: Revised Departmental Guidance on Valuation of Travel Time in Economic Analysis | US Department of Transportation, Washington, DC, USA, 2016.

West Attica Region: Restoration of damages for the local community of Kineta. West Attica's Technical Works Observatory., 2021.

Xu, H.: Modification of normalised difference water index (NDWI) to enhance open water features in remotely sensed imagery, International Journal of Remote Sensing, 27, 3025–3033, https://doi.org/10.1080/01431160600589179, 2006.